Suppression of premature capacity loss by methods based on the gel–crystal concept of the PbO$_2$ electrode

D. Pavlov

Central Laboratory of Electrochemical Power Sources, Bulgarian Academy of Sciences, Sofia 1113 (Bulgaria)

Abstract

Based on experimental data, the concept has been developed recently that positive active mass (PAM) agglomerates comprise not only crystal zones but also hydrated gel zones. The latter are built of linear hydrated polymer chains that interconnect the crystal zones and have both electron and proton conductivity. The reasons for the premature capacity loss (PCL) of batteries has been looked for in: (i) decrease in the electroconductivity of the gel zones due to the lack or insufficient content of dopants (tin, antimony, etc.) that improve the contacts between the polymer chains and interconnect them into an integral system with high electron and proton conductivity; (ii) decrease in the PAM density on pulsation of the plate upon cycling, leading to a decrease in concentration of polymer chains in the gel that interconnect the agglomerates to form the skeleton of the PAM; (iii) decrease in degree of hydration of the corrosion layer, which is important for both its flexibility and its ability to take on the mechanical stresses that are created as a result of oxidation of the grid metal. Based on the gel–crystal concept of the PAM, technological methods have been suggested for suppressing the phenomena that cause PCL (er.g., use of 4PbO·PbSO$_4$ (4BS) pastes, high-temperature curing, addition of dopants such as tin and antimony to the grid alloys, etc.). The role of the corrosion layer in suppressing PCL has been disclosed and especially the significance of the stoichiometric coefficient n of PbO$_n$ $(1 < n < 2)$ in the layer, as well as the factors that give rise to an increase in the value of this parameter. The stoichiometric coefficient exerts an influence on both the electroconductivity of the corrosion layer and the rate of its interaction with H$_2$SO$_4$. Appropriate selection of grid-alloy additives (antimony, tin, etc.) give rise to increases in the rate of oxidation of PbO to PbO$_n$ in the corrosion layer, the value of the stoichiometric coefficient n, and the degree of hydration of the corrosion layer. All these effects will result in the suppression of the phenomena of PCL. Based on the gel–crystal concept, some design methods have also been suggested to alleviate PCL. Thus, solving the problems related to PCL is only possible when design and technological methods are applied in combination.

Introduction

Premature capacity loss
   When lead–antimony alloys that are used for the production of positive lead/acid battery grids are substituted by lead–calcium counterparts, the capacity of lead dioxide plates declines rapidly on cycling. This phenomenon has been called the 'antimony free effect', 'premature capacity loss' (PCL), 'early capacity decline' or 'relaxable

insufficient mass utilization' (RIMU). The term PCL is used here. Attempts have been made to associate the cause of this phenomenon with change in the properties of the positive active mass (PAM) or/and of the corrosion layer (CL) during cycling. Several concepts have been proposed to account for the PCL effect, namely:

(i) changes in the resistance of the contacts between the PbO_2 crystals of the PAM during cycling;

(ii) changes in the intrinsic electrochemical activity of the PAM during cycling (hydrogen-loss model);

(iii) changes in the abundance ratio of the α- and β-modifications of PbO_2;

(iv) formation of a $PbSO_4$ barrier layer;

(v) formation of a PbO passivation layer;

(vii) formation of cracks in the CL.

These possibilities have been discussed in recent surveys [1, 2].

A thorough analysis of the above concepts of PCL shows that each of them has its place in the battery theory and is well supported by experimental evidence [2]. That is why a search was made for a more general phenomenon that would unite all these concepts, i.e., the latter would refer to different aspects of the general phenomenon. The processes causing PCL were related to the gel–crystal structure of PAM and CL [2, 3]. The aim of the present paper is to suggest technological and design methods for suppressing the phenomena of PCL and, thus, for prolonging battery life, based on the principal conclusions of the gel–crystal concept. In this sense, it is a continuation of the work reported in ref. 2. In a future paper, a report will be given of methods for suppressing PCL during battery operation, from the point of view of the same concept.

Gel–crystal structure of PAM

Figure 1 presents a transmission electron microscope (TEM) photograph of parts of a PAM agglomerate. The dark zones have an α-PbO_2 or β-PbO_2 crystal structure, while the light regions are composed of amorphous and hydrated $PbO(OH)_2$ [4]. The latter are built of hydrated linear polymer chains that have both electron and proton conductivity:
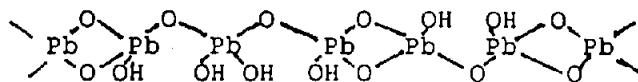
The crystal zones are degenerated n-type semiconductors and are sized between 200 and 700 Å. These dimensions provide large surface area, high reactivity and high electroconductivity. The high deficiency and mobility of the crystal lattice ensure good interaction with the hydrated gel zones that surround them. The latter are in dynamic equilibrium with crystal zones; the relaxation time is very short.

High-resolution TEM observations of the gel zones reveal linearly arranged, hydrated polymer chains in the agglomerates (Fig. 2). Arranged planes of polymer chains are clearly seen in the encircled regions. The distances between the chains range from 10 to 15 Å. These values are considerably larger than the interplanar distances in the elementary cell. This indicates that there is water between the planes. In the other regions, polymer chains are folded chaotically.

Electrons and protons move along the polymer chains in the gel zones that connect the crystal zones and thus create both electron and proton conductivity in PAM. Gel zones have a higher resistance than the crystal zones. This resistance depends on the
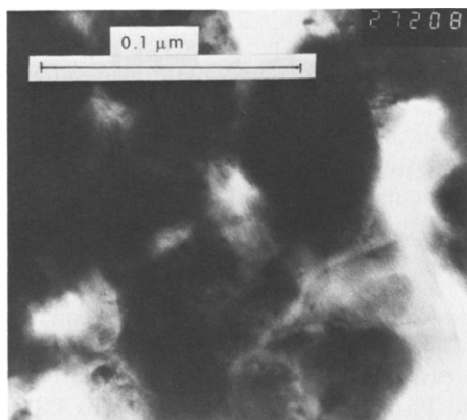
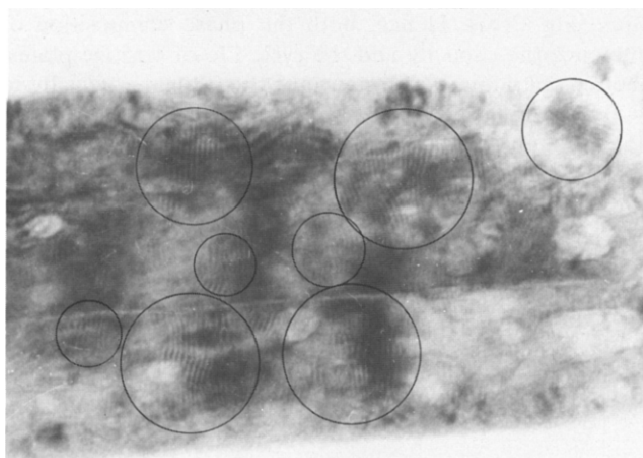Fig. 1. TEM photographs of parts of PAM agglomerates.

Fig. 2. High-resolution TEM micrograph of parts of agglomerates. Encircled zones feature linearly arranged hydrated polymer chains. The interchain distance is 10 to 15 Å.

concentration of polymer chains in the gel. Furthermore, gel zones influence the mechanical properties of the PAM. Based on these concepts of the structure of PAM, the work reported here examines possible methods for suppressing the phenomena that cause PCL.

Influence of the technology for positive-plate production on the suppression of PCL

Effect of paste phase-composition on plate capacity

The production of positive plates comprises the following technological procedures:

(i) *Paste preparation and pasting of the grids*. Leady oxide is thoroughly mixed with water and H_2SO_4. Basic lead sulfates are obtained. When the process is conducted

at temperatures lower than 65 °C, $3PbO \cdot PbSO_4 \cdot H_2O$ (3BS) is produced. At temperatures above 70 °C, the result is $4PbO \cdot PbSO_4$ (4BS) crystals.

(ii) *Plate curing*. During the curing of the plates, oxides and basic lead sulfates in the paste are recrystallized and become interconnected to form a skeleton. The grid metal corrodes and the resulting oxide layer is connected to the skeleton of the paste. The lead contained in the paste is also oxidized.

(iii) *Formation of PAM*. Through electrochemical reactions, the cured paste is oxidized to PbO_2-active material. The matrix of the paste skeleton is transformed to the structure of the active mass. Lead oxide and basic lead sulfate crystals are converted into agglomerates of PbO_2 particles.

What is the effect of the above-mentioned technological procedures on the capacity and the cycle life of positive plates? Figure 3 presents the capacity performance of batteries that have been assembled with positive plates prepared with 3BS and 4BS pastes and using Pb–6wt.%Sb–0.1wt.%As and Pb–1.6wt.%Sb–0.1wt.%As grids [5].

The batteries prepared with 4BS pastes and high-antimony grids exhibit a slightly lower initial capacity, but a considerably longer cycle life (Fig. 3(a)). When the low-antimony grids are used, the plates pasted with 4BS pastes have higher capacity than those prepared with 3BS pastes (Fig. 3(b)). Hence, both the phase composition of the paste and the grid alloy influence the capacity and the cycle life of positive plates. The 4BS technology ensures better operating performance of the plates, especially in the case of those produced with low-antimony grids.

Electron micrographs of the PAM obtained from 3BS and 4BS pastes are presented in Fig. 4. The agglomerates of 4BS-based PAM are tens of μm in size, while those resulting from 3BS pastes have dimensions between 1 and 3 μm. This difference in size is due to the fact that 4BS crystals are much larger than 3BS ones and their matrices are reproduced in the PAM agglomerates.
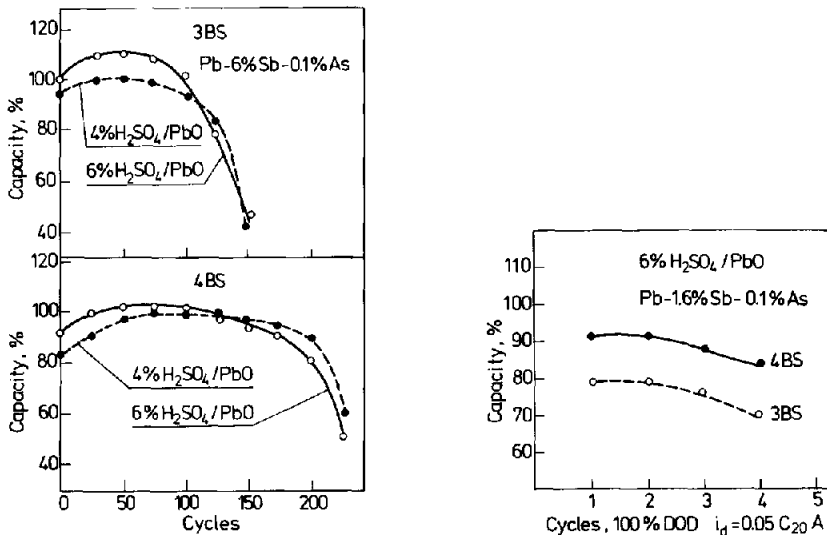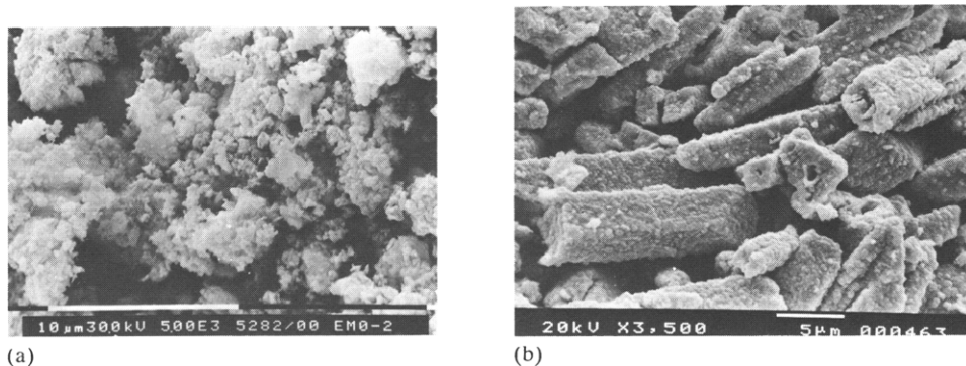

Fig. 3. Changes in capacity of 12 V/42 Ah batteries (produced with positive plates with 3BS and 4BS pastes) during cycling at the C_{20} rate. The capacity-limiting factor is the positive plates [5].

Fig. 4. Electron micrographs of PAM obtained from: (a) from $3PbO \cdot PbSO_4 \cdot H_2O$ (3BS) pastes; (b) from $4PbO \cdot PbSO_4$ (4BS) pastes.
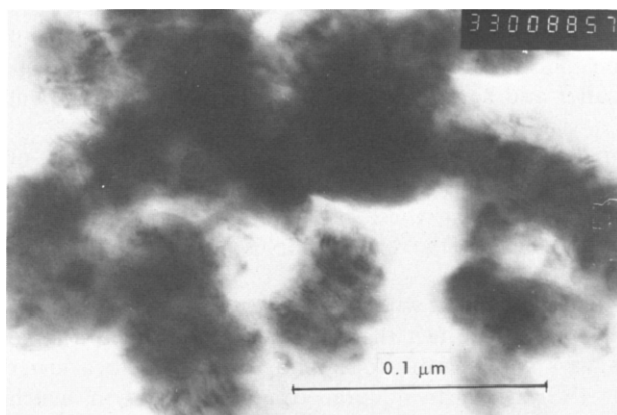
Fig. 5. TEM micrograph of the contact between agglomerates and PAM.

Figure 5 shows TEM micrographs of parts of the agglomerates at the sites of contact between them. At these locations, a lower mass density is observed. This indicates that these regions are hydrated. The decrease in density of the gel zones is due to a decrease in the concentration of the polymer hydrated chains that connect the crystal zones. When the concentration is decreased, the ohmic resistance in these zones increases. Agglomerates that are interconnected through gel zones with a low concentration of the polymer chains would be excluded from the current-generation process, especially if the gel concentration is below a certain critical value. This would result in a decline in capacity.

No physical boundaries are formed between the agglomerates or particles of the PAM skeleton, but rather their gel and/or crystal zones coalesce. On fusion of the gel zones of two agglomerates, the polymer chains of one gel zone merge with the polymer chains of the other to form a common chain. The current passes through the thus formed 'bridge' between the two agglomerates. Hence, the PAM skeleton is a continuous system that is comprised of elements with different resistances. Crystal zones have low resistance (degenerated semiconductor), while the resistance of gel zones depends on: (i) the concentration of the parallel polymer chains that interconnect the crystal zones; (ii) the mobility of electrons along these chains.

On plate discharge, the concentration of the polymer chains in a number of gel zones may decrease below a certain value and, thereby, cause parts of the PAM to be excluded from the current-generation process. This may happen at the sites of linkage between particles and agglomerates. Surface forces would try to concentrate the gel again and thus maintain the process of current generation. On the other hand, these surface forces may lead to breaking of the contact between particles and agglomerates.

When the cross section of the contact area between two agglomerates is sufficiently large (as is the case of the PAM obtained from 4BS pastes), it is more probable that it will contain crystal zones rather than gel zones (the latter amount to about 30% in PAM). With decrease in the cross section of the contact areas between agglomerates there is an increased probability that they will contain gel zones. When the cross section is reduced below a certain critical value, the contact between the agglomerates is realized only through gel zones. This is because crystal zones are always covered by a gel layer and such layers on adjacent agglomerates become in contact with one another (Fig. 5). Moreover, the concentration of gel zones in the bulk of the agglomerates is higher than that on the surface. Large agglomerates will have a greater content of gel zones with a high polymer chain concentration. Furthermore, the number of contacts between agglomerates will be smaller and hence the probability of disintegration will be lower.

The above conclusions from the gel–crystal concept imply that the skeleton of the PAM obtained from 3BS pastes may readily disintegrate into smaller parts that, in turn, may shed from the plate. By contrast, these processes are much slower in the skeleton of 4BS-based PAM and, hence, the battery life is considerably longer (Fig. 3(a)).

Figure 3(a) also shows that plates produced with 4BS pastes have a low capacity at the beginning of cycling. This is due to the fact that the 4BS crystals have a large size and, consequently, do not always undergo full formation. This leads to a lower initial capacity for the plate. For 4BS crystals to undergo complete oxidation, which would yield full plate capacity, 10 to 40 charge/discharge cycles are often needed.

Effect of grid-alloy additives (dopants) on energy performance of plates

Figure 3 shows that the concentration of antimony in the grid alloy affects strongly the capacity of plates. According to the gel–crystal concept, this effect is due to the incorporation of antimony ions into the gel zones [4]. These ions improve the connections between the linear polymer chains that form the network. A schematic representation of these connections is presented in Fig. 6.

Both antimony and tin ions have high affinity towards water. Polymer chains, on their part, are hydrated. Consequently, both antimony and tin ions would be readily bonded to hydrated polymer chains to form a polymer network. It is therefore appropriate to term these dopants 'binders'. Binders support the polymer chains and prevent the polymer network from disintegration on decrease of the PAM density.

When there is no binder, the polymer network exhibits high conductivity only with a high density of polymer chains in the gel. With decreasing PAM density, the polymer chains disintegrate rapidly and the conductivity of the gel zones declines abruptly. This happens upon cycling of the plates. The sensitivity of the conductivity of the gel, without binder, on the density of the PAM is one of the reasons for PCL. The same effect is also observed when the concentration of the binders in the gel is low. Most sensitive to these changes are the regions near the CL/PAM interface.
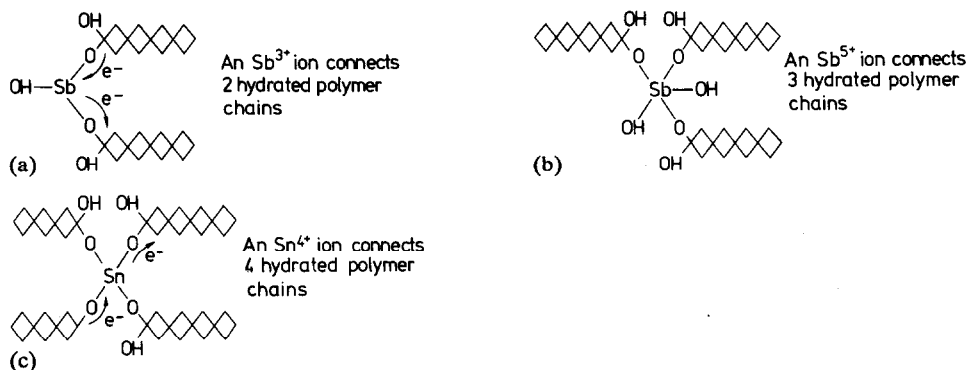
(a)

OH

O
OH—Sb
O

e⁻
e⁻

OH

An Sb³⁺ ion connects
2 hydrated polymer
chains

(b)

OH OH

O O
Sb—OH
O O

OH

OH

An Sb⁵⁺ ion connects
3 hydrated polymer
chains

(c)

OH OH

O O
Sn
O O

e⁻

e⁻

OH

An Sn⁴⁺ ion connects
4 hydrated polymer
chains

Fig. 6. Schemes for the connections between hydrated polymer chains in gel zones through Sb^{3+}, Sb^{5+} and Sn^{4+} ions into an integral system with electron and proton conductivity.
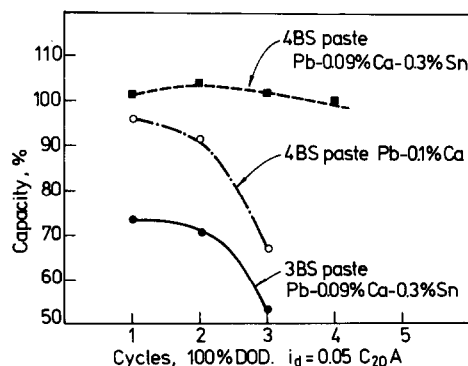
Fig. 7. Capacity data for positive plates produced with 4BS and 3BS pastes and lead–calcium grids with different tin content [6].

Fortunately, these regions are saturated with ions of the binder that are formed as a result of oxidation of the grid alloy.

The above discussion can be summarized as follows: antimony improves the electron conductivity of the gel, and the tendency of antimony towards hydration both stabilizes the gel concentration and improves the proton conductivity; similar properties are exhibited by tin and bismuth, and probably by other metal ions as well.

The effect of tin on the capacity and cycle life of batteries produced with lead–calcium grids is illustrated in Fig. 7 [6].

Plates produced with Pb–0.09wt.%Ca–0.3wt.%Sn grids and 3BS pastes have a capacity of 75%, while the capacity of plates with Pb–0.12wt.%Ca grids (without Sn) and 4BS pastes is 95%. The advantage of the 4BS pastes is obvious. When 0.3 wt.% of Sn is added to the grid alloy of plates prepared with 4BS pastes, their capacity is increased to 104% and this value is quite stable during cycling with 100% depth-of-discharge (DOD). Tin ions are incorporated into the gel zones of the PAM agglomerates and enhance the mobility of electrons and protons between the crystal zones (Fig. 6). This will improve and stabilize the electroconductivity of the gel zones in the skeleton and, thus, will keep the PAM in a state of uniform current generation.

The tendency of tin to reduce the resistance of positive battery plates has been reported by Giess [7] and is illustrated in Fig. 8. When charged plates with lead grids are strongly polarized, the presence of 1.6 wt.% Sb and 0.6 wt.% As in the alloy decreases the electrode polarization. The addition of 0.6 wt.% Sn to the lead alloy has an even stronger effect and reduces by almost twice the polarization of the plate. Tin ions are readily hydrated. Thus, their influence on gel zones is similar to that of antimony ions (Fig. 6).

Komaki [8] has studied the changes in inner resistance of the positive plate of 2 V/1.2 Ah elements as a function of overcharge. Tin was introduced into the grid alloy at different concentrations or the grid was coated with a tin-rich layer. Figure 9 presents the changes in inner resistance of the battery (as determined by the positive plate) during overcharge. A low and stable resistance of the plate on battery overcharge is sustained for a long period only when tin is applied as a coating over the grid. Most probably, with this technology, the gel zones in the agglomerates at the CL/PAM interface are saturated very quickly with tin ions and the latter are entrapped there for greater periods. Furthermore, tin reduces the resistance of the
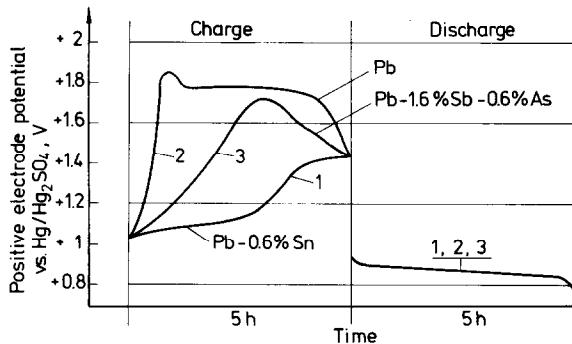

Fig. 8. Potential vs. time curves for positive plates with different grid alloys during charge [7].
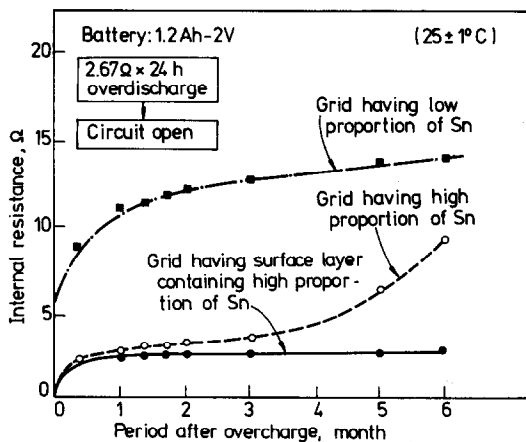

Fig. 9. Changes in inner resistance of plates produced with grids containing different amounts of tin in the alloys or with lead grids with a tin-rich coating during overcharge of 2 V/1.2 Ah battery [8].

CL which is composed of PbO_2 and PbO_n $(1<n<2)$ agglomerates. Takahashi et al. [9] have established that a tin-rich coating on the grid surface is very effective in avoiding passivation of positive plates with lead–calcium grids. This effect will be discussed in more detail below.

It can now be concluded that it is not sufficient to have a given alloy additive (tin, antimony, etc.) introduced into the grid alloy, but that the concentration and position in the interface of this additive are also important. Multilayered grids are more efficient in suppressing the phenomena that cause PCL. These investigations indicate also that the interface CL/PAM is the plate-building element that is the most sensitive to the action of dopants.

Effect of plate-curing conditions on CL/PAM contact

The active material of an automotive-battery plate has a surface area of 500 to 700 m^2. The surface area of the grid is of the order 30 to 60 cm^2. The current generated as a result of the electrochemical reaction on 700 m^2 area is concentrated in the PAM near the ribs of the grid and passes through the CL and the 60 cm^2 grid surface. This makes the structure of the CL and of the adjacent PAM regions the most critical elements in the positive plate.

The CL and its contact with the PAM are formed during the procedures of pasting and, especially, curing of the plates. Curing continues for 48 to 72 h and is conducted at high temperature and humidity. Under these conditions, metal oxidation is accelerated. The corrosion processes result in the formation of a layer of lead oxide. This layer provides the connection with the skeleton of the cured paste. On plate formation, first, the CL is oxidized to PbO_n $(1<n<2)$ and PbO_2, and then the cured paste is oxidized. During battery operation, the CL grows in thickness and changes in phase composition. The behaviour depends on the operating conditions. It should be expected that the curing conditions would affect the initial composition of the CL and its contact with the PAM. Plate curing is conducted at: (i) 40–65 °C — low-temperature curing; (ii) above 75 °C — high-temperature curing.

Rand and Lam [10] have studied the dependence of the capacity on the number of cycles for batteries with positive plates prepared with 3BS pastes (low-temperature curing) and 4BS pastes (both conventional and advanced curing procedures at high temperature). The results obtained are presented in Fig. 10. The advanced high-
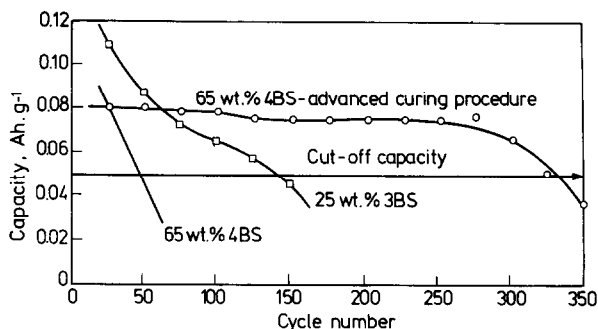

Fig. 10. Capacity performance. The test is performed according to the requirements of the JIS 5361 standard. Positive plates are produced with 3BS pastes. On low-temperature curing, the skeleton of the cured paste is built of 3BS, and on high-temperature curing the cured paste consists of 4BS crystals [10].
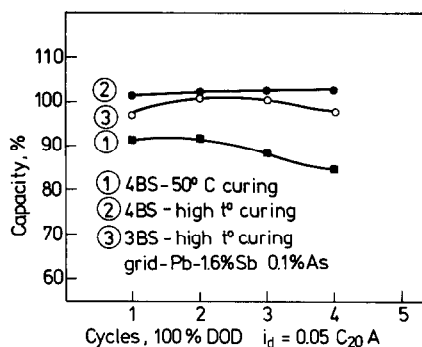
Fig. 11. Capacity at 50% utilization of the active mass of plates produced with different initial pastes and under different curing conditions.

TABLE 1

Corrosion weight losses of plates during high- and low-temperature curing

Curing conditions	Weight loss $(10^{-5}\ g\ h^{-1}\ cm^2)$
45 °C, 72 h	1.3
90 °C, 48 h	5.3

temperature curing procedure improves significantly battery cycle life. Similar results have also been obtained in the author's laboratories [6].

The reason for the beneficial effect of the high-temperature curing procedure may be looked for both in the recrystallization of 4BS pastes and in the processes occurring at the metal/CL/PAM interface. Figure 11 presents the capacity data for the first four cycles (20-h discharge) for plates prepared with 4BS and 3BS pastes cured at high temperatures [6]. Plates produced with 4BS pastes and cured at 50 °C have a capacity of 91%. If the same plates are cured at high temperatures (appropriate mode), the capacity increases to 103%. Plates prepared with 3BS pastes and cured at high temperatures also exhibit capacity higher than 100%. This indicates that the positive effect of curing is mainly due to the enhanced rate of the processes occurring at the grid/paste interface, under the action of high temperature, and is less dependent on the nature of the paste.

We have determined the rates of corrosion of Pb–1.6wt.%Sb–0.1wt.%As plates, pasted with 4BS pastes, on curing at 45 °C for 72 h and at 90 °C for 48 h. These data are presented in Table 1. On high-temperature curing, a much thicker CL is formed. The presence of such a layer is a prerequisite for the formation of a good contact between the grid and the PAM. Hence, high-temperature curing can be used as a method for suppressing the phenomena leading to PCL.

Effect of the CL on battery performance

Reactions associated with CL growth

During battery operation, the metal grid of the positive plate is oxidized both by the evolved oxygen and by the self-discharge processes. This results in a growth of

the CL thickness. The phase composition of the CL is determined by the following reactions:

$$Pb \xrightarrow{V_1} PbO \tag{1}$$

$$PbO \xrightarrow{V_2} PbO_n \quad (1 < n < 2) \tag{2}$$

$$PbO_n \xrightarrow{V_3} PbO_2 \tag{3}$$

where V_1, V_2 and V_3 are the rates of the respective reactions.

It has been established, through scanning electron microscope (SEM) observations, that the CL is built of agglomerates and particles of various sizes and forms. Their composition depends on the ratio between the rates of the above three reactions, namely $V_1:V_2:V_3$. Thus:

(i) when $V_1 > V_2$, a distinct PbO sublayer is formed and the electrode system is of the type Pb/PbO/PbO$_n$/PbO$_2$; as PbO has a high ohmic resistance, this electrode is passivated;

(ii) when $V_1 < V_2$, the electrode system Pb/PbO$_n$/PbO$_2$ is formed. PbO$_n$ has low ohmic resistance and hence the electrode is electrochemically active; the positive battery plate is a system of this type.

Structure of CL

Figure 12 presents, schematically, the structure of the Pb/CL/PAM interface of the PbO$_2$ plate. The CL is comprised of the following components:

(i) A dense (or inner) sublayer that isolates the metal surface from the solution and thus slows down the process of grid corrosion. The inner CL may be composed either of PbO$_n$ ($n \geqslant 1.5$) in which case the electrode has low ohmic resistance, or of PbO whereby the electrode is passivated.

(ii) A porous (or outer) sublayer composed of PbO$_n$ and PbO$_2$. This layer is in contact with the electrolyte. In order to have low ohmic resistance, the contact area (S) of the porous sublayer with the active mass should be much larger than that at the interface with the pore solution, i.e., $S_{CL/PAM} \gg S_{SL/pore \ solution}$. Another factor that determines the ohmic resistance of the interface is the stoichiometric coefficient of the PbO$_n$ sublayer. That is why the properties of the PbO$_n$ sublayer are of crucial importance to the performance of positive battery plates and the occurrence of the PCL effect.
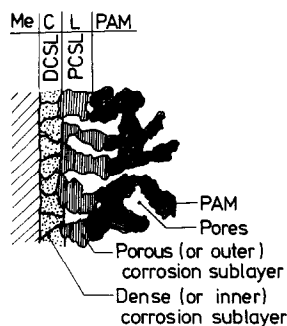

Fig. 12. Schematic representation of the structure of the CL.

Effect of stoichiometric coefficient on PbO_n electroconductivity

The dependence of the specific electroconductivity on the stoichiometric coefficient of the lead oxides is presented in Fig. 13 [11]. When the stoichiometric coefficient of the lead oxide reaches values between 1.4 and 1.5, the oxide electroconductivity becomes equal to that of PbO_2. Hence, to ensure that positive plates yield high power and capacity, the PbO_n sublayer of the CL formed on the grids should have a stoichiometric coefficient that is > 1.4.

Figure 14 presents the dependence of the stoichiometric coefficient of the CL on the potential of pure-lead electrodes [12]. When the potential of the lead dioxide electrode is more positive than 1.45 V (versus a Hg/Hg_2SO_4 reference electrode), the stoichiometric coefficient of the CL reaches values higher than 1.5.

The stoichiometric coefficient is influenced by additives to the grid alloy. Table 2 summarizes the values of the CL stoichiometric coefficient with respect to the antimony content of the grid alloy [13]. Equivalent data for lead–silver alloys [14] are given in Table 3. While antimony maintains high values of the stoichiometric coefficient ($n = 1.6$–1.85) of the CL, silver decreases this coefficient within the range 1.5–1.6. The
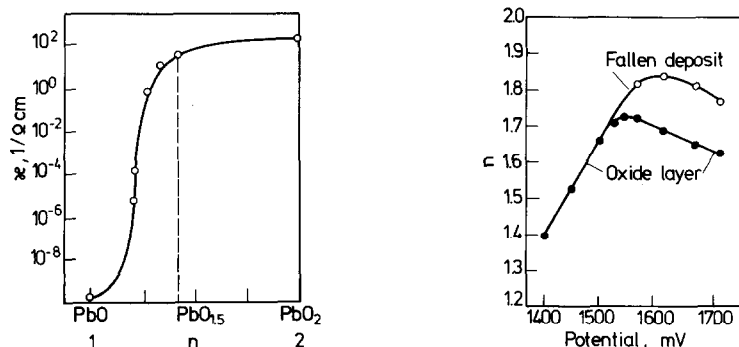

Fig. 13. Dependence of PbO_n specific electric conductivity on the stoichiometric coefficient, n [11].

Fig. 14. Dependence of the stoichiometric coefficient, n, of the anodic layer on the oxidation potential [12].

TABLE 2

Dependence of stoichiometric coefficient, n, in CL on antimony content in lead–antimony electrodes [13]

wt.% Sb	0.5	4.9	7.3	10.6
n	1.40–1.75	1.60–1.75	1.65–1.75	1.75–1.85

TABLE 3

Dependence of stoichiometric coefficient, n, in CL on silver content in lead–silver electrodes [14]

wt.% Ag	0.05	0.10	0.28	0.65	1.0	3.0
n	1.50	1.55	1.55	1.57	1.60	1.60

overall stoichiometric coefficient of the CL on lead–arsenic electrodes varies between 1.40 to 1.65. This suggests that arsenic, like silver, inhibits the oxidation of PbO to PbO_2. Electrodes with lead–silver grids are known to exhibit a tendency to passivation.

Effect of grid-alloy additives on the potential and rate of the $PbO \rightarrow PbO_n$ reaction

Through linear potentiodynamic sweeps (SLV), studies have been made [15–17] of the effect of tin, antimony and bismuth additives on the potential at the start of the $PbO \rightarrow PbO_n$ reaction. First, polarization of a lead–antimony electrode at 0.6 V is conducted and the electrode system $Pb/PbO/PbSO_4$ is formed as a result. Then, a series of potential sweeps between 0.6 and 1.3 V are performed (Fig. 15(a)) to determine the potential at which the oxidation of PbO commences, and the stoichiometric coefficient of PbO_n increases to $PbO_{(n+k)}$ $(k>0)$ [15]. This potential is denoted by arrows in Fig. 15(a). The encircled number indicates the number of the potential sweep. Figure 15(b) presents the dependence of the potential of PbO oxidation on the number of potential sweeps for lead–antimony electrodes with different antimony contents [15].

Antimony has an electrocatalytic effect that enables the reactions of oxidation, $PbO \rightarrow PbO_n$ and $PbO_n \rightarrow PbO_{(n+k)}$ $(k>0)$, to start at a lower potential (Fig. 15). Antimony causes the value of n to increase quickly. This leads to an abrupt increase in the CL conductivity and, thus, the current generated by the above reactions for one and the same number of sweeps is much higher in antimonial electrodes than in pure-lead counterparts (Fig. 15(a)). Figure 16 presents analogous data to Fig. 15(b) for tin [16]. The effect of tin is similar to that of antimony.

Bismuth, too, has an electrocatalytic effect on the above reactions [17]. Consequently, certain alloying additives such as antimony, tin and bismuth (and probably some others, too) act as electrocatalysts for reaction (2) and thus maintain $V_2 > V_1$. This ensures a high stoichiometric coefficient for the PbO_n sublayer of the CL, and thus maintains
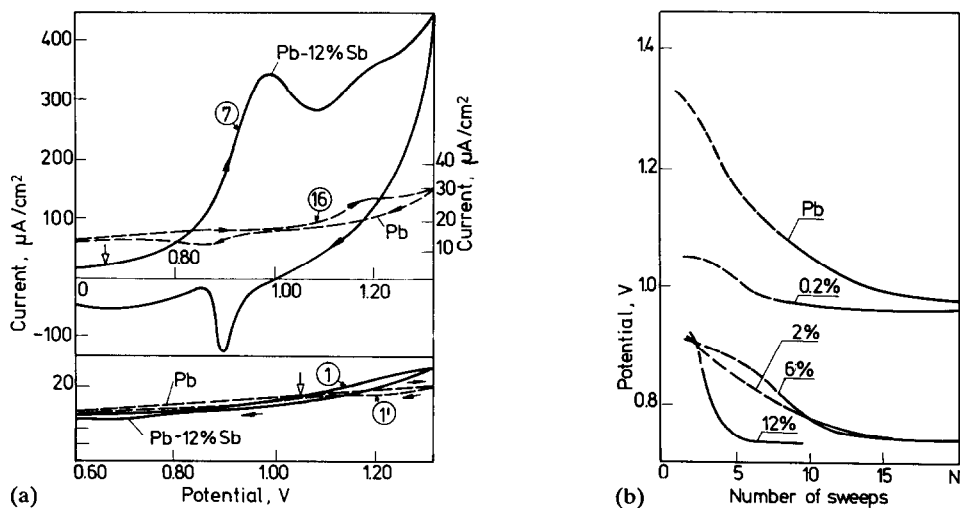

Fig. 15. (a) SL voltammograms at sweeps up to 1.3 V. The arrow marks the start of PbO and PbO_n oxidation. Encircled numbers denote the consecutive number of the sweep. Sweep rate 10 mV s^{-1} [15]. (b) Dependence of the potential at which oxidation of PbO and PbO_n commences on the number of sweeps for different lead–antimony electrodes [15].
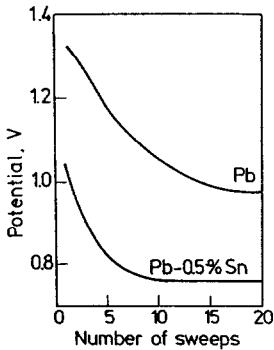
Fig. 16. Dependence of the potential at which oxidation of PbO or PbO_n starts on the number of sweeps for lead and Pb–0.5wt.%Sn electrodes [16].

a high conductivity for the CL over a considerably wider potential range below the equilibrium potential of the $PbO_2/PbSO_4$ electrode. This improves the utilization of the PAM during the process of current generation.

Chemical behaviour of PbO_n sublayer

PbO_n may be regarded as a mixed oxide that consists of PbO and PbO_2. When the PbO_n sublayer of the CL becomes in contact with the H_2SO_4 solution, the following disproportionation reaction takes place:

$$PbO_n + H_2SO_4 \rightarrow kPbO_2 + s(mPbO \cdot PbSO_4) + qPbSO_4 \qquad (4)$$
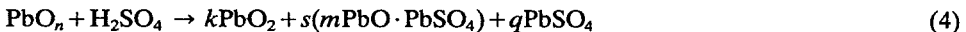
The formation of PbO_2 in the CL is beneficial to the operation of the battery. The $mPbO \cdot PbSO_4$ and $PbSO_4$ phases have dielectric behaviour and, hence, are most undesirable. This is why reaction (4) should be avoided, or suppressed, during battery operation. This can be achieved in the following ways:

(i) A high value of n is maintained. In this case the amounts of the $PbSO_4$ and $mPbO \cdot PbSO_4$ phases in the CL would be negligible. As mentioned before, antimony and tin act as electrocatalysts for the oxidation of PbO, and antimony keeps the value of n above 1.75.

(ii) The pH of the solution in the CL pores is kept above 6.5. $PbSO_4$ is thermodynamically unstable in neutral and alkaline pH regions. Consequently, no $PbSO_4$ will be formed in these regions. This can be accomplished by:
• reducing the radii of the pores in the CL to sizes that are smaller than those of the membrane pores [18, 19]; this would lead to alkalization of the solution in the CL pores
• increasing the plate thickness and thus slowing down the flow of H_2SO_4 to the CL; this would lead to loss of battery power [20]
• selecting such a ratio between the active materials, H_2SO_4:Pb:PbO_2, so that only a weak flow of H_2SO_4 would reach the CL and only after the positive plate has reached the desired DOD; the quantity of H_2SO_4, however, should be sufficient not to limit the capacity.

The role of the proportion between H_2SO_4 and the lead and PbO_2 active materials is illustrated in Fig. 17. By placing different numbers of positive and negative plates into the same volume of H_2SO_4 solution, the proportion between the electrolyte and the lead and PbO_2 active masses is significantly changed (Fig. 17 (a), (b)). Figures
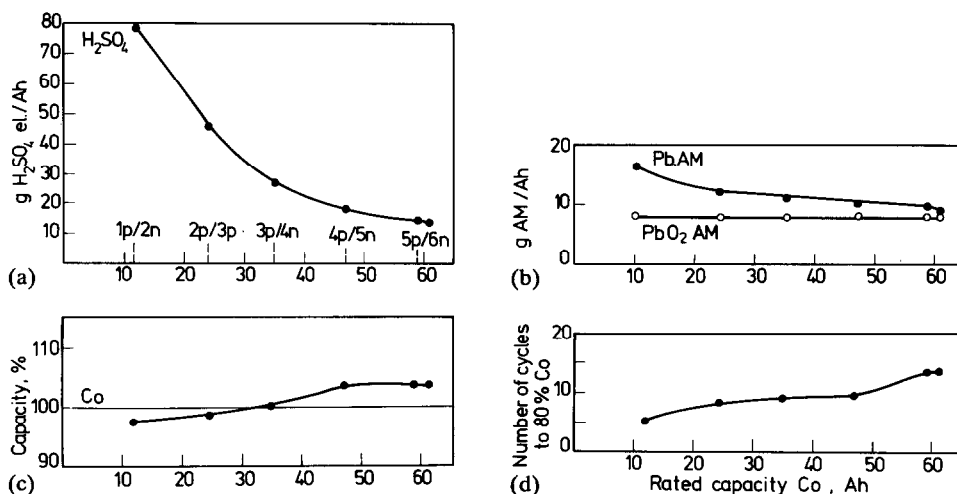
Fig. 17. (a), (b) Dependence of g active material/Ah and g H_2SO_4 electrolyte/Ah on the rated capacity of cells assembled with different numbers of positive and negative plates; (c) capacity exhibited by the above cells; (d) number of cycles endured at 100% DOD at $i = 0.05$ C_{20} A until 80% of the rated capacity is reached.

17 (c) and (d) show the results from the capacity measurements and the number of cycles at 100% DOD with $i_d = 0.05$ C_{20} A [6]. When the amount of H_2SO_4 in the cell decreases below 19 g electrolyte/Ah the capacity and cycle life of the plates increase. Hence, there is a certain amount of electrolyte that yields optimum battery capacity and life. It has been established [18] that on deep-discharge cycling of batteries with lead–tin–calcium grids the battery capacity decreases almost linearly with the increase in concentration of H_2SO_4 in the cells from 1.1 to 1.2 sp. gr.

From the above discussion, it follows that the proportion between the electrolyte and the lead and PbO_2 active materials plays an important role in suppressing the sulfation of the CL.

Anti-crack effect of gel zones in the CL

It has been established that the hardness of the CL obtained on a Pb–4wt.%Sb grid in the PbO_2 potential region is 54 kg mm^{-2}, and that of the CL on a Pb–0.09wt.%Ca grid is 88 kg mm^{-2} [21]. These results indicate that alloying additives influence the composition of the CL or affect its hydration. The dependence of the degree of CL hydration on the antimony content in the grid alloy has been determined, see Fig. 18 [15].

Antimony increases the number of gel zones in the CL and this leads to a decline in hardness of the latter. The PAM is 30–35% hydrated [22]. The CL on pure-lead electrodes is ~10% hydrated (Fig. 18). This significant difference in the degree of hydration will affect the mechanical and physical properties of the CL/PAM interface.

Upon oxidation of lead, the volume of the resulting PbO is 20% greater than that of the initial lead. This creates inner stresses in the CL that promote the formation of cracks. The number of cracks are much less on lead–antimony electrodes than on
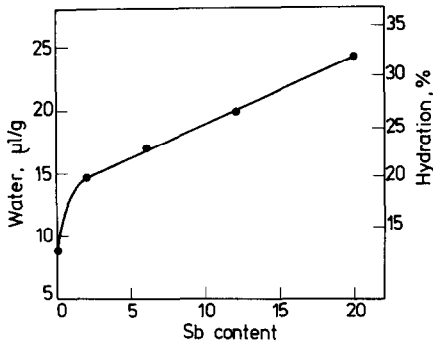
Fig. 18. Dependence of the water content (μl g^{-1}) or the degree of hydration (%) of the CL on the content of antimony in the lead–antimony grid alloy [15].

lead–calcium ones [23]. The cracks tend to be located radially on lead–antimony grids and concentrically on lead–calcium grids [24].

Cracks have a two-fold effect. On one hand, they decrease the cross section of the contact area through which the current passes at the PAM/CL interface, and on the other hand they play the role of channels through which H_2SO_4 can more readily reach the most critical zone in the plate and create conditions for reaction (4) to proceed.

Gel zones in the particles and agglomerates of the CL can accommodate the mechanical stresses and dissipate the mechanical energy that is accumulated. In this way, the gel zones serve as 'hinges' and provide increased flexibility to the CL/PAM structure. This creates a reliable contact between the plate grid and the PAM.

Design of lead/acid cells and the gel–crystal concept

The presence of gel zones in the PAM structure creates a dynamic structural element in the plate that can respond to the volume changes in the structures of the PAM and the CL and thus lower the rate of disintegration during battery charge and discharge.

Reduction of PbO_2 results in the formation of $PbSO_4$. The latter has a 65% greater molar volume than that of PbO_2. This creates inner mechanical stresses in the PAM. The gel zones dissipate this mechanical energy. On charge and discharge, the plate pulsates. During this process, the volume of the plate and the surface area of the PAM do not always return to their initial states.

Figure 19 presents data on the pore volume, the plate thickness, the apparent density and the BET surface area of the PAM after 5 and 30 cycles [25]. The PAM is produced from 4BS, 3BS and PbO pastes. The density of the PAM decreases on plate cycling. It has been established that when the density of the active mass falls below a certain critical value (~ 3.4 g cm^{-3}), the structure of the PAM is very difficult to restore upon plate charge and some regions of the plate are excluded from the current-generation process [25]. As a consequence, the plate capacity declines. To avoid this situation, the pulsations of the PAM should be restricted. This can be achieved by confining the plate within a given volume (for example by placement of the PAM in tubes) or by subjecting the battery plates to the action of a force that would counteract to pulsation. Takahashi et al. [26] have determined the changes in
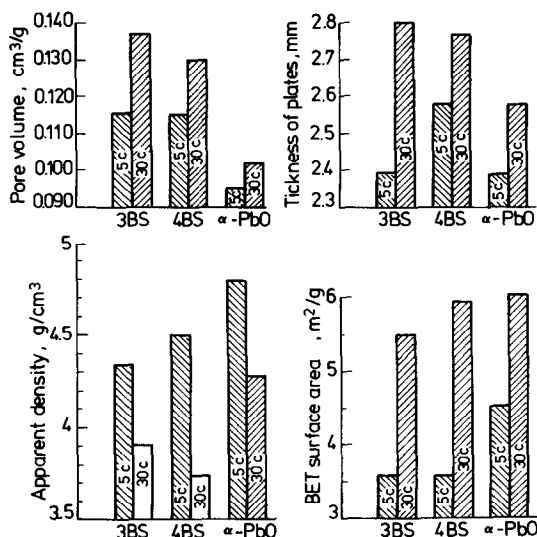
Fig. 19. Comparative data on pore volume of PAM, thickness of the positive plate, apparent density and BET surface area of PAM obtained from 3BS, 4BS and α-PbO pastes at the 5th and 30th cycle. All data are for charged plates [25].

capacity, electrical resistance and thickness of the positive plate on cycling when a force of 0.2 or 1.0 kg cm^{-2} is applied to the cell (Fig. 20). The cells under higher pressure exhibit smaller increase in thickness, lower ohmic resistance, higher capacity and longer life. When the pressure over the plates is increased from 0.2 to 0.4 kg cm^{-2}, the cell life is increased by a factor of two. The ability of the plate to pulsate on cycling is restricted to about 15%. Hence, the life of the battery is very sensitive to changes in the PAM density.

Dopants play a major role in suppressing the PCL effect. When introduced in sufficient amounts, they may compensate for the effects of decreased density or may maintain a reliable contact between the CL and the PAM, as well as improve the conductivity of the nonstoichiometric oxides in the CL. This is why any decrease in the concentration of dopants, or their absence altogether, will have a dramatic effect on PCL.

It has been established that the crystallinity of the paste increases with paste density [27]. It is probable that the gel zones with higher water-content undergo dehydration. This means that polymer chains in the zones with highest ohmic resistance will become concentrated.

The gel zones are in dynamic equilibrium with both the crystal zones and the solution in the PAM pores. When the PAM density increases, the radii of the pores decrease. This impedes the access of the different ions to the micropores of the agglomerates, which, in turn, causes a change in the composition of the contained solution. The equilibria between the solution and the gel zones, and between the gel and crystal zones are changed as well. Thus, PAM density, which is a purely physical (mechanical) parameter, can affect the physicochemical processes that occur in the agglomerates. An increase in the PAM density may change the concentration of polymer chains in the gel zones and, hence, the capacity of the plate will change. When a certain pressure is exerted upon the PAM, the density of the gel zones will be maintained
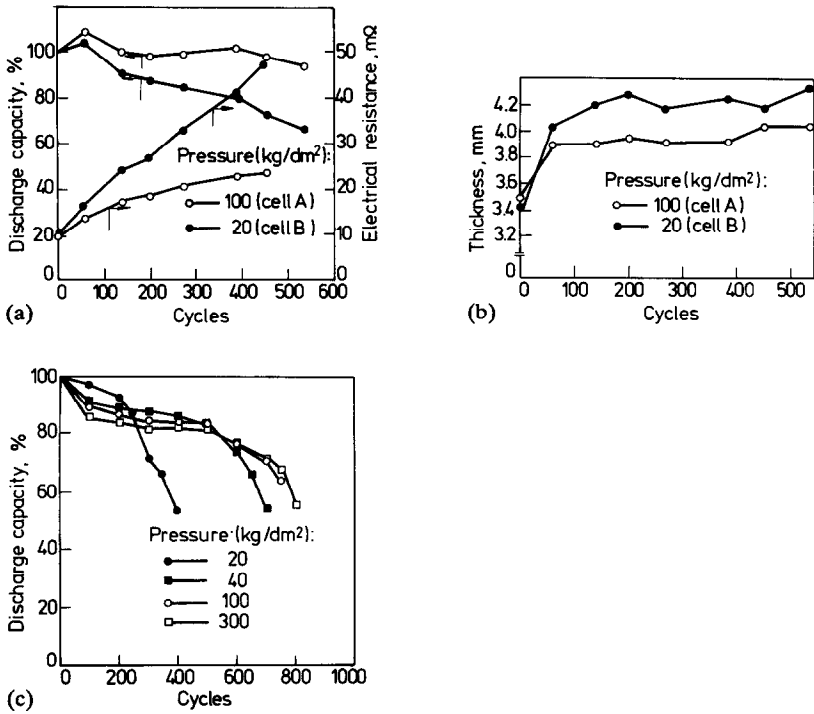
Fig. 20. (a) Changes in capacity and electrical resistance during cycling of cells under pressure of 100 and 20 kg dm^{-2}; (b) dependence of positive plate thickness on the number of cycles for cells under pressure of 100 and 20 kg dm^{-2}; (c) dependence of capacity on the number of cycles for cells under different pressures [26].

above a given value, and thus a decrease in their conductivity will be prevented. This will ensure high plate capacity over greater periods of battery operation.

Conclusions

Following the experimental demonstration of gel zones in the PAM [3, 22, 28], it has become essential to examine the influence of these zones on the behaviour of the PAM and the CL. A most valuable outcome of the gel–crystal concept would be the securing of an explanation for the phenomena that give rise to PCL. The latter is a difficult problem and has been tackled by researchers and manufacturers for many years. Further, derivation of such an explanation, should allow methods to be suggested for the suppression of PCL phenomena and, hence, for improving the cycle life of positive battery plates.

The above study, based on the gel–crystal concept, presents an attempt at revealing, in depth, the phenomena leading to PCL as well as their mechanisms. The following methods for suppressing the phenomena can now be suggested:

Methods related to production technology

(i) Selection of appropriate binders that would interconnect the polymer chains in a network and would keep the conductivity of the gel zones high. Such

additives are antimony and tin. A search should be made for other, more effective, binders.

(ii) Selection of appropriate dopants to the grid alloy that maintain a high stoichiometric coefficient and a high conductivity in the PbO_n layer. Such additives are antimony and tin.

(iii) Increase in the concentration of gel zones in the PAM agglomerates and improvement of the contact between them through incorporation of large agglomerates in the PAM skeleton. This can be achieved by using 4BS pastes.

(iv) Improvement of the contact between the grid and the PAM (paste) through formation of a thick CL, e.g., by high-temperature curing of the plates.

Methods related to cell design

(i) Restriction of plate pulsation to about 10–15% during charge and discharge. This would reduce the rate of decrease in the gel-zone density upon cycling and would maintain higher plate capacity.

(ii) Limitation of the amount of H_2SO_4 to below 19 g electrolyte/Ah in order to reduce sulfation of the CL.

The simultaneous application of these methods is expected to lengthen significantly the life of batteries with low-antimony and antimony-free grids.

References

1 A. Hollenkamp, *J. Power Sources, 36* (1991) 567–585.
2 D. Pavlov, *J. Power Sources, 42* (1993) 345–363.
3 D. Pavlov, *J. Electrochem. Soc., 139* (1992) 3075–3080.
4 D. Pavlov and I. Balkanov, *J. Electrochem. Soc., 139* (1992) 1830–1835.
5 G. Papazov and D. Pavlov, *Annual Report 1975* CLEPS-BAS; D. Pavlov, in B.D. McNicol and D.A.J. Rand (eds.), *Power Sources for Electric Vehicles,* Elsevier, Amsterdam, 1984, p. 333.
6 D. Pavlov, St. Ruevski and T. Rogachev, in preparation.
7 H.K. Giess, in K.R. Bullock and D. Pavlov (eds.), *Proc. Symp. Advances in Lead–Acid Batteries,* The Electrochemical Society, Pennington, NJ, USA, 1984, Vol. 84-14, pp. 241–251.
8 A. Komaki, *Report 1992,* Shin–Kobe Electric Machinery Co., Ltd., Tokyo, 1992.
9 K. Takahashi, H. Yasuda, N. Takami, S. Horie and Y. Suzui, *J. Power Sources, 36* (1991) 451–460.
10 D.A.J. Rand and L.T. Lam, *The Battery Man,* (Nov.) (1992), p. 19.
11 F. Lappe, *J. Phys. Chem. Solids, 23* (1962) 1563.
12 D. Pavlov and T. Rogachev, *Electrochim. Acta, 23* (1978) 1237.
13 T. Rogachev, *J. Power Sources, 23* (1988) 331.
14 D. Pavlov and T. Rogachev, *Electrochim. Acta, 31* (1986) 241.
15 B. Monahov and D. Pavlov, *Ext. Abstr., Proc. Int. Conf. on Lead/Acid Batteries: LABAT '93, St. Konstantin, Varna, Bulgaria, June 7–11, 1993,* Abstr. No. 16, p. 61.
16 D. Pavlov, B. Monahov, M. Maja and N. Penazzi, *J. Electrochem. Soc., 136* (1989) 27.
17 M. Bojinov and D. Pavlov, *Ext. Abstr., Proc. Int. Conf. on Lead/Acid Batteries: LABAT '93, St. Konstantin, Varna, Bulgaria, June 7–11, 1993,* Abstr. No. 19, p. 72.
18 H. Nakashima and S. Hattori, *Proc. Pb80 Int. Lead Conf., Madrid, Spain, 1980,* pp. 86–97.
19 J. Garche, *J. Power Sources, 30* (1990) 47–54.
20 T.G. Chang, in K.R. Bullock and D. Pavlov (eds.), *Proc. Symp. Advances in Lead-Acid Batteries,* The Electrochemical Society, Pennington, NJ, USA, 1984, Vol. 84-14, pp. 86–97.
21 S. Hattori, M. Yamashita, M. Kono, M. Yamane, N. Nakashima, J. Yamashita and J. Nakayama, *ILZRO Project LE-276, Rep. No. 5,* 1980.
22 D. Pavlov, I. Balkanov, T. Halachev and P. Rachev, *J. Electrochem. Soc., 136* (1989) 3189.

23 B.K. Mahato, *J. Electrochem. Soc., 126* (1979) 365.
24 D.C. Constable, J.K. Gardner, J.A. Hamilton, K. Harris, R.J. Hill, D.A.J. Rand, S. Swan and L.B. Zalcman, *J. Power Sources, 23* (1988) 257.
25 D. Pavlov and E. Bashtavelova, *J. Electrochem. Soc., 133* (1986) 241–248.
26 K. Takahashi, M. Tsubota, K. Yonezu and K. Ando, *J. Electrochem. Soc., 130* (1983) 2144–2149.
27 D. Pavlov, A. Dakhouche and T. Rogachev, *J. Power Sources, 30* (1990) 117–130.
28 D. Pavlov, I. Balkanov and P. Rachev, *J. Electrochem. Soc., 137* (1987) 2390–2398.